Heliyon 10 (2024) e24008

Contents lists available at ScienceDirect

Heliyon

journal homepage: www.cell.com/heliyon

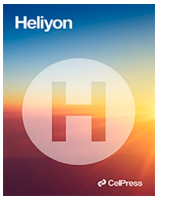

Aconitum coreanum alleviates cerebral ischemic stroke through the PI3K/Akt signaling pathway in gerbils model

Ru Jia, Qian Cai *, Yang Qu **

College of Pharmacy, Liaoning University of Traditional Chinese Medicine, Dalian, China

ARTICLE INFO

Keywords:
Cerebral ischemic stroke
Aconitum coreanum
Compound absorbed into blood
Bioinformatics
PI3K/Akt signaling pathway

ABSTRACT

Cerebral ischemic stroke (CIS) is a kind of acute cerebrovascular disease with fast onset, low-cure rate, and high case-fatality rate. The application of *Aconitum coreanum* on CIS was recorded in many ancient books in China with it mechanism and effective components unclear. This study aimed to analyze the potential mechanism and effetvie components of *A. coreanum* on treating CIS. Neurological function score, cerebral infarction rate, and inflammatory indicators were applied to evaluate the efficacy of *A. coreanum* on gerbils with CIS. The prototype compounds in *A. coreanum* which were absorbed into blood was analyzed and identified by Ultra high performance liquid chromatography-Q exactive focus-Mass spectrometer (UPLC-QE-MS). And bioinformatics analysis was used to predict their potential targets or pathways of action. Western blotting and immunofluorescence were adopted to validate the targets or pathway with high relation. After treatment with *A. coreanum*, the neurological function status of gerbils with CIS was significantly improved, the ischemic area of the brain and the levels of inflammatory indicators significantly reduced. 22 prototype compounds in *A. coreanum* absorbed into blood were identified mainly including C-20 and C-19 diterpenoid alkaloids. Gene ontology (GO) function enrichment analysis illustrated that *A. coreanum* acted on protein phosphorylation, receptor complexes, protein kinase activity, and inflammatory response to impove CIS. The kyoto encyclopedia of genes and genomes (KEGG) pathway enrichment analysis results revealed that PI3K/Akt signaling pathway was a key pathway. Western blotting and immunofluorescence validated that *A. coreanum* acted on PI3K/Akt signaling pathway. In conclusion, *A. coreanum* improved the inflammantory condition in CIS by acting on PI3K/Akt signaling pathway and the effective components were the diterpenoid alkaloids in it.

1. Introduction

Cerebral ischemic and intracerebral hemorrhage induced cerebral stroke (CS), which was also known as apoplexy in the theory of traditional Chinese medicine. According to the Global Burden of Disease Study (GBD) survey in 2019, CS has become the third leading cause of death in the world, with more than 6.37 million premature deaths attributed to CS [1]. Cerebral ischemic stroke (CIS) was the most common type of CS in clinical practice, and epidemiological investigation showed that approximately 69.6 %~70.8 % of patients sufferred from CS in China were caused by cerebral ischemic, i.e. CIS [2]. CIS patients exhibited symptoms such as facial paralysis,

* Corresponding author.
** Corresponding author.
E-mail addresses: caiqianmail@sina.com (Q. Cai), quyang_7@aliyun.com (Y. Qu).

https://doi.org/10.1016/j.heliyon.2024.e24008
Received 24 July 2023; Received in revised form 18 December 2023; Accepted 2 January 2024
Available online 5 January 2024

glossolalia, blurred vision, nausea and vomiting, which seriously affected the patient's normal life and also caused certain distress to their family members [3].

Traditional Chinese medicine has a long history in treating CIS, which can effectively alleviating pain and inflammation, improving activity limitation, and quality of life [4–8]. Ac*onitum coreanum* (Lèvl.) Rapaics belonged to the Ranunculaceae family, the root of which has the effects of dispelling dampness and cold, and relieving pain [9]. *A. coreanum* was first documented in Supplementary Records of Famous Physicians as herbal medicine [10]. Many ancient books recorded the use of *A. coreanum* in the treatment of CIS [11]. According to the Yuqiu Medicine Solution, *A. coreanum* could expel wind and relieve dampness, expel obstruction and promote phlegm. It was also applied to treat stroke, aphonia, and nasal deviation [12]. Qianzheng San is a classic formula treating CIS, with *A. coreanum* as the main component [13]. Although it has been reported in ancient books and used in clinical, the anti-CIS pharmacological substances and mechanism of it were still unclear.

In our study, gerbils with CIS was used as model to evaluate the efficacy of *A. coreanum,* Ultra high performance liquid chromatography-Q exactive focus-Mass spectrometer (UPLC-QE-MS) was used to indentify the compounds of *A. coreanum* absorbed into blood, while bioinformatics was used to screen the key targets of them, which was further validated by western blotting and immunofluorescence. This manuscript aimed to explore the effect of *A. coreanum* on CIS and its potential mechanisms.

2. Materials and methods

2.1. Medicinal materials

The dried root of *A. coreanum* (Lèvl.) Rapaics, which was collected from the Liaoning Xifeng planting base of Traditional Chinese Medicine and was identified by Professor Liang Xu. Naoluotong was purchased from local pharmacy (Zhejiang CONBA Pharmaceutical Co., Ltd. lot: 210401).

2.2. Animals and treatment

Thirty two male Mongolian gerbils (12 weeks old, weight 80 ± 10 g) were provided by the Experimental Animal Center of Harbin Medical University [No. SCXK (Hei) 2013-001]. All gerbils were allowed to freely access food and water. All animal studies were approved by the Animal Ethics Committee at the Affiliated Hospital of Liaoning University of Traditional Chinese Medicine (Approval No. 2019 YS (DW) -028-0).

After one week of adaptive feeding, gerbils were randomly divided into Sham surgery group (SG), model group (MG), positive drug group (PG) and *A. coreanum* group (AC), with 8 gerbils in each group. Except the gerbils in SG, gerbils of the other groups were unilateral ligated the right carotid artery to create the CIS model. Gerbils were anesthetized by intraperitoneal injection of pentobarbital sodium (40 mg/kg), fixed on the operating table in a supine position. The skin in front of the neck was depilated, and disinfected. A longitudinal incision was made along the neck, with a length of 1 cm. The subcutaneous tissue, soft tissue, and adipose tissue were separated layer by layer to expose the right common carotid artery and vagus nerve. The right common carotid artery was separated with a glass needle, the artery was ligated with cotton thread. The wound was sutured, and finally disinfected. SG performed the same steps as the surgery group, except for not ligating the right carotid artery.

After successful modeling, the gerbils of AC were orally administered the powder suspension of *A. coreanum* (0.586 mg/g), and those of PG were orally administered the suspension of Naoluotong in water (0.390 mg/g), while other groups were orally administered saline, for fourteen consecutive days. After the last administration, the gerbils were anesthetized with 1 % pentobarbital sodium (0.15 mL/100 g). And blood was taken from abdominal aorta, centrifuging at 3500 rpm [1235 (× g)] for 15 min, plasma were collected and stored at −20 °C for the determination of biochemical indices. After cardiac perfusion, the brains of the gerbils were collected., part was frozen in a refrigerator at −80 °C for protein expression measurement, part was fixed in neutral formaldehyde for immunofluorescence, and the other part was frozen in a refrigerator at −20 °C for 30 min, and were sliced into 2 mm thick coronal section for 2,3,5-triphenyltetrazolium chloride (TTC) staining.

Table 1
Scoring standard of neurological function of gerbil.

Behavior	Score
Stand posture	0 point: Being able to stand completely upright; 1 points: Being able to stand but with head tilted; 2 points: Being able to stand, but with both the head and upper body tilted; 3 points: Failing to stand or falling immediately after standing.
Facial expression	The eyes cannot be opened normally, the nose is crooked, and the head unconsciously leans to one side. 1 point will be awarded for each item that meets the criteria.
Flexibility of action	0 point: Being able to act flexibily; 1point: Being able to act normally, but falling after a few times; 2points: Cannot jump high and fall immediately while climbing; 3 points: Unable to jump or climb.

2.3. Neurological evaluation

Gerbils of each group was scored for neurological deficits to assess their neurological function, on the day before modeling and the third, seventh, fourteenth days after modeling. The scoring standard of neurological function was listed in Table 1. The higher the score, the severer the neurological deficits of the gerbils.

2.4. TTC staining

The brain slices were placed in 2 % TTC solution under 37 °C for 30 min. After carefully washed with physiological saline to remove the staining solution, photos were taken and the cerebral infarction area of gerbils in different treatment groups were determined by image J 1.51 and calculated by the formula following. Cerebral infarction rate = (ischemic contralateral hemisphere area - ischemic non infarct area)/ischemic contralateral hemisphere area × 100 %]

2.5. Determination of biochemical indices

The levels of inflammatory factors including interleukin-6 (IL-6) and tumor necrosis factor-α (TNF-α) in plasma and brain homogenate of the gerbils were measured by enzyme-linked immunosorbent test kit according to the procedure outlined in the manual supplied by Shanghai Lianshuo Biotechnology Co., Ltd. (lot: 202206).

2.6. Identification of prototype compounds of *A. coreanum* absorbed into blood

100 mg powder of *A. coreanum* was extracted by 500 μL 80 % methanol, centrifugated at 12000 rpm [13800 (× g)] for 15 min. The supernatant was filtered by 0.22 μm microporous membrane filtration to obtain sample solution of *A. coreanum*.

Gerbils were divided into control group (CG) and *A. coreanum* group (AG), with 6 gerbils in each group. After one week of adaptive feeding, the gerbils of AG group was given the powder of *A. coreanum* suspened in saline at dosage of 5.060 mg/g, while the gerbils of CG group was given physiological saline for five consecutive days. One hour after the last administration, gerbils in each group were anesthetized with 1 % pentobarbital sodium (0.15 mL/100 g), and blood was taken from abdominal aorta. After centrifugated at 3500 rpm [1235 (× g)] for 15 min plasma was collected. 40 μL hydrochloric acid (2 mol/L) and 1600 μL acetonitrile were added to 400 μL plasma successively. After vortex mixing thoroughly, the mixture was centrifugated at 12000 rpm [13800 (× g)] for 5 min and 1800 μL supernatant was taken and blown dry, then reconstituted by 150 μL 80 % methanol. The solution was filtered by 0.22 μm microporous membrane filtration to obtain samples.

LC-MS/MS analysis was performed on an UPLC system (Vanquish, Thermo Fisher Scientific) with a Waters UPLC BEH C18 column (1.7 μm 2.1 × 100 mm). The sample injection volume was set at 5 μL. The flow rate was set at 0.5 mL/min. The mobile phase consisted of 0.1 % formic acid in water (A) and 0.1 % formic acid in acetonitrile (B). The multi-step linear elution gradient program was as follows: 0–11 min, 85 %∼25 % A; 11–12 min, 25 %∼2 % A; 12–14 min, 2 % A.

An Q Exactive Focus mass spectrometer coupled with an Xcalibur software was employed to obtain the MS and MS/MS data based on the IDA acquisition mode. During each acquisition cycle, the mass range was from 100 to 1500 , and the top three ions of every cycle were screened and the corresponding MS/MS data were further acquired. Sheath gas flow rate: 45 Arb, Aux gas flow rate: 15 Arb, Capillary temperature: 400 °C, Full ms resolution: 70000, MS/MS resolution: 17500, Collision energy: 15/30/45 in NCE mode, Spray Voltage: 4.0 kV (positive).

2.7. Bioinformatics analysis

Under the condition of probability >0, target prediction was performed on the prototype compounds of *A. coreanum* absorbed into blood using the Swiss Target Prediction database and Pharmaper database. The collected target information was corrected to standard gene names using the Uniprot database. The results of the Swiss Target Prediction database and Pharmaper database were summarized and duplicate targets were removed to obtained 658 targets.

The keyword "cerebral ischemic stroke" was used to search and screen potential targets for CIS in the GeneCards database, DisGenet database, and Uniprot database. Finally, after summarizing the targets obtained from the above databases and excluding duplicate ones, 4736 stroke related targets were obtained.

String database was used to construct a protein-protein interaction (PPI) network. The core targets and key pathways were analyzed and screened based on the built-in Network Analyzer of Cytoscape 3.7.2, and the component-target-pathway network was constructed.

2.8. Western blotting

100 mg brain tissue was added by 1000 μL radio immunoprecipitation assay (RIPA) lysis buffer (Beyotime, lot: No.042121210726). After homogenizing, centrifugated at 12000 rpm [13800 (× g)], 4 °C for 15 min, and the protein content in the supernatant was determined by bicinchoninic acid (BCA) reagent kit (Beyotime, lot:P0010). After transferring the protein onto the polyvinylidene fluoride (PVDF) membrane, the membrane was sealed in 5 % skimmed milk for 1 h, and then it was incubated with PI3K (Abcam, lot: GR3360941-15, 1:1000), Akt (CST, lot:28, 1:1000), *p*-Akt (CST, lot:7, 1:1000) overnight at 4 °C. After incubating by horseradish

peroxidase (HRP) labeled secondary antibody (Affinity, lot:AH11286487, 1:5000) for 1 h, the membrane was developed with electrochemiluminescence (ECL) luminescent solution. Chemiluminescence imaging system was used to image and take photos, and the relative protein expression was calculated by image J 1.51.

2.9. Immunofluorescence

After fixed and incubated with rabbit anti-PI3K (Abcam, lot:GR3369948-2, 1:150) and mouse anti-*p*-Akt (CST, lot:1, 1:200) at 4 °C overnight, the brain sections were incubated with fluorescein isothiocyanate-labeled goat anti-rabbit antibody (abcam, lot: GR3375958-2, 1:800) or goat anti-mouse antibody (abcam, lot:GR3399161-2, 1:800) for 1 h at room temperature in the dark. After stained with a resin sealant containing 6-diamino-2-phenylindole (DAPI) (biosharp, lot:22047869), the sections were observed using a fluorescence microscope (Nikon, Ti2).

2.10. Statistics analysis

Statistical Package for the Social Sciences program (SPSS 17.0) was used to statistically analyze the data, and the values were expressed as mean ± standard deviation ($\bar{x} \pm s$). Those conforming to normal distribution were analyzed by one-way analysis of variance (ANOVA), and the least significant differenc (LSD) method was used for comparison between groups; the Kruskal-Wallis method of rank sum test was used for comparison between groups not conforming to normal distribution. Statistical significance was defined as a *P*-value <0.05.

3. Results

3.1. A. coreanum improved the symptoms of gerbils with CIS

After unilateral ligated the right carotid artery, the neurological function score of gerbils significantly increased ($P < 0.001$), indicating the successful replication of the CIS model. Compared to MG, after three day of administration of *A. coreanum*, the score significantly decreased ($P < 0.01$), and continued declining during the treatment of *A. coreanum* in the following days (Fig. 1).

TTC staining indicated that after treatment with *A. coreanum*, the cerebral infraction area in gerbils partially recovered, and the cerebral infarction rate decreased from 52.61 % to 23.74 %, with a significant difference compared to MG ($P < 0.001$) (Fig. 2A and B).

The results of biochemical indicators determination indicated that compared to MG, there was a significant decrease of TNF-α and IL-6 in AC and the trend was same into blood and brain ($P < 0.001$) (Fig. 3).

4. Prototype components of A. coreanum were absorbed into blood

Total ion current chromatograms of *A. coreanum* and blood were obtained by UPLC-QE-MS (Fig. 4A–C). A total of 80 compounds were tentatively identified from *A. coreanum* according to the reported literature and relevant databases (Table 2). Among them, 22 prototype compounds were detected in drug-contained plasma including C-20 diterpenoid alkaloids, such as Guanfu base A, Hetisine, Acoridine, etc., and C-19 diterpenoid alkaloids, such as Isotalatizidine, Condelphine, and Talatizamine, as well as saccharides and organic acids.

A. coreanum regulated PI3K/Akt signaling pathway in the treatment of CIS based on bioinformatics analysis.

Among the targets of prototype compounds absorbed into blood and targets of CIS, 318 targets were in common (Fig. 5). Those were imported into the String database to construct a PPI network (Fig. 6). Based on the analysis of the Network Analyzer built-in in Cytoscape 3.7.2, 112 highly active targets were screened. The mechanism of *A. coreanum* in treating CIS might be related to these

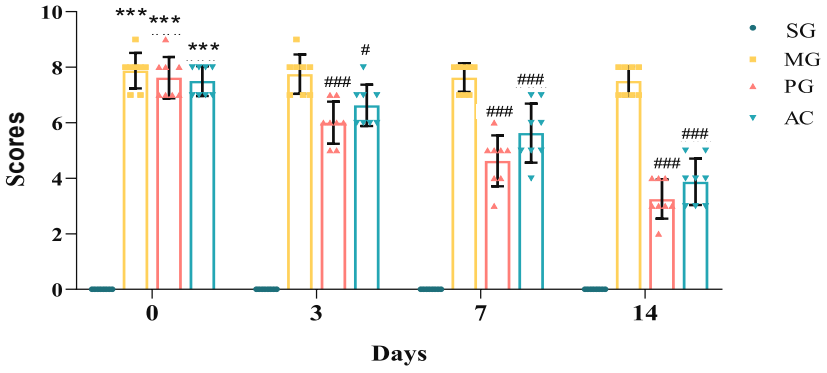

Fig. 1. Neurological function score of gerbils in each group
(Compared with SG, ***$P < 0.001$; Compared to MG, $^{\#}P < 0.05$, $^{\#\#\#}P < 0.001$).

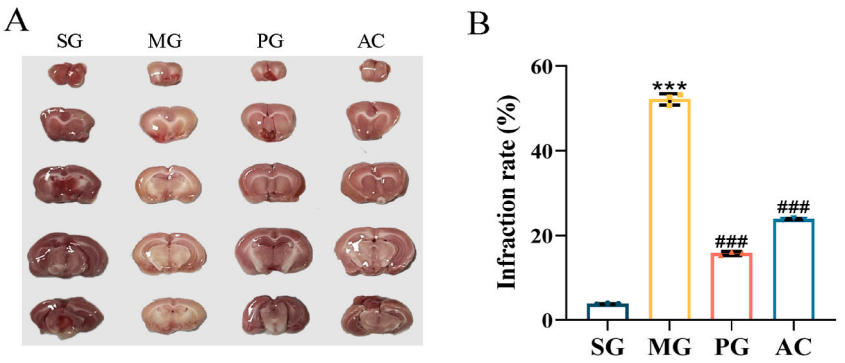

Fig. 2. Infraction of brain of CIS gerbils A.Results of TTC staining; B: Results of infraction rate (Compared with SG, ***$P < 0.001$; Compared to MG, $^{\#\,\#\,\#}P < 0.001$).

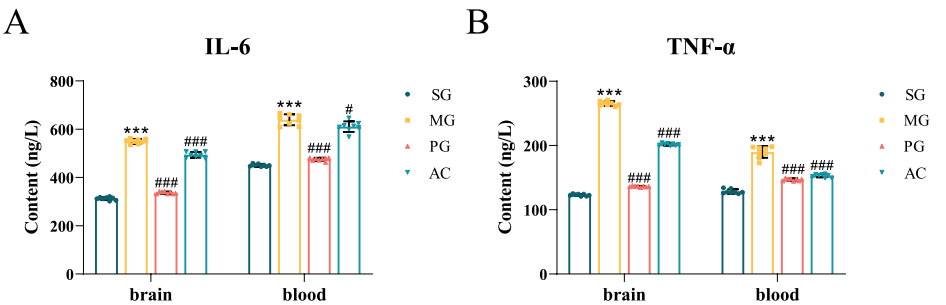

Fig. 3. Content of biochemical indicators in brain and blood. A:Content of IL-6 in brain and blood; B:Content of TNF-α in brain and blood (Compared with SG, ***$P < 0.001$; Compared to MG, $^{\#}P < 0.05$, $^{\#\,\#\,\#}P < 0.001$).

proteins.

Gene ontology (GO) function enrichment analysis was carried out for core targets, and the top 20 of them including biological processes (BP), cell composition (CC) and molecular functions (MF) were selected to draw a visual bar chart (Fig. 7). The analysis results predicted that the potential impact of *A. coreanum* on treating CIS were protein phosphorylation, receptor complexes, protein kinase activity, and inflammatory response.

The kyoto encyclopedia of genes and genomes (KEGG) pathway enrichment analysis results were arranged in ascending order of *P*-values, and the top 20 pathways were selected to draw a bubble chart (Fig. 8). The results predicted that the correlation between PI3K/Akt signaling pathway and the treatment on CIS of *A. coreanum* were significant, indicating that it might be a key pathway for the treatment of CIS with *A. coreanum*.

A total of 292 nodes (22 constituents, 112 targets and 158 pathways) and 2752 edges made up the constructed constituent-target-pathway network using Cytoscape 3.7.2. The darker the color and larger the shape, the higher the degree value (Fig. 9). The network diagram displayed that Guanfu base A, Guanfu base Q, Guanfu base Z, Coreanine C, and Coreanine A acted on AKT, N-methyl-laurotetanine, Condelphine, Coreanine C, Coreanine A, and Triacetylhetisine acted on PI3K. The results indicated multiple interaction between the active ingredients of *A. coreanum* and CIS targets.

To verify the results of bioinformatics analysis, the expression of proteins involved in PI3k/Akt pathway were determined by westen blotting.The results were calculated using Image J 1.51 to obtain the grayscale values of the band, and the relative expression was illustrated with column chart (Fig. 10A and B). The results showed that compared with SG, the expression of PI3K and *p*-Akt in MG significantly reduced ($P < 0.05$). This indicated that a successful modeling was established and also indicated that CIS affected the expression of related proteins in the PI3K/Akt pathway. Compared with MG, the expression levels of PI3K and *p*-Akt in AC significantly increased ($P < 0.05$).

PI3K and *p*-Akt could be detected and quantified at the surface of gerbils brain slices by immuno-fluorescence staining (Fig. 11A and B). The nuclear staining showed that there were a large number of cells in the hippocampal CA1 area of gerbils in SG, and the neurons arranged orderly, compacted in structure, completed in cell morphology, which indicated that the neurons in the hippocampal CA1 area of gerbils in SG were healthy. However, there were fewer cell in those in MG, and the arrangement of neurons were irregular, with loose structure, incomplete cell morphology, indicating that the neurons were damaged. After treatment with *A. coreanum*, the number of cells in the CA1 area of the hippocapus increased, which arranged in an orderly manner, with relative compact structures. Most of the cells had intact morphology indicating that *A. coreanum* maintained the integrity of neurons and protected them from ischemic injury.

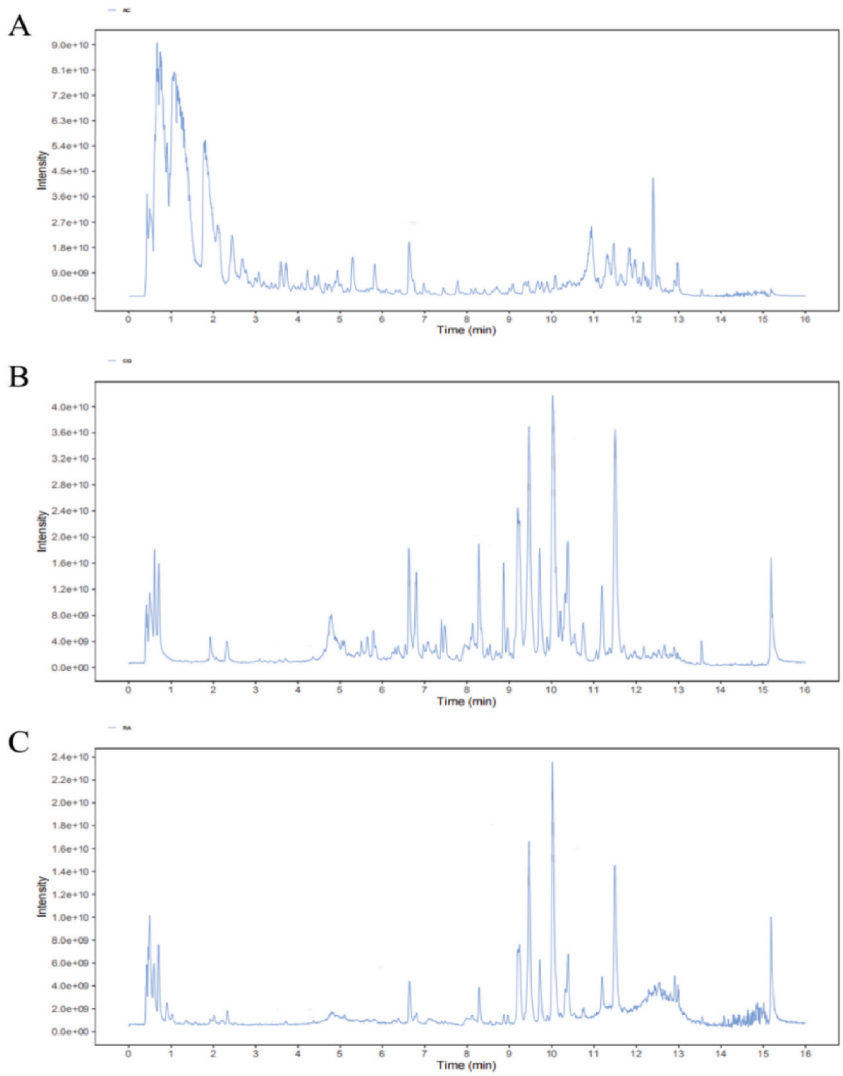

Fig. 4. Total ion current chromatograms of *A. coreanum* and blood. A: *A. coreanum* B: blood of CG C: blood of AG.

The expression of PI3K and *p*-Akt in hippocampal CA1 neurons could be fully expressed in SG, while the expressions of those in MG reduced. After the treatment of *A. coreanum*, the expression of them in AC increased.

5. Discussion

CIS is caused by various factors that result in insufficient blood supply to brain. Ischemia and hypoxia lead to irreversible ischemic necrosis or softening of local brain tissue, which mainly manifests as a series of neurological functional deficits in clinical practice [26]. The brain injury in the acute phase of CIS is mainly caused by the damage of ischemia and hypoxia to brain tissue. This process is accompanied by cell apoptosis, autophagy, oxidative stress, and inflammatory. In modern clinical practice, brain damage caused by thrombosis were treated from three aspects: thrombolysis, antiplatelet aggregation, and lowering blood lipids by ateplase, aspirin, statins, etc [27–29]. The damage caused by CIS also involves various pathways such as oxidative stress and inflammatory, in which used as adjunctiue therapy.

Modern research has shown that the alkaloid components in *A. coreanum* are related to anti-arrhythmias, improving atrial fibrillation, and affecting Na^+/K^+ channels, etc. Studies have shown that the diterpenoid alkaloids from *A. coreanum* had anti-arrhythmic effects on cardiac sodium current [30], the total alkaloids from *A. coreanum* were correlation with atrial fibrillation [31], Guanfu base A and Guanfu base G had effect on HERG K^+ channel [32]. As a commonly used traditional Chinese medicine in clinical practice, *A. coreanum* also has a long history and good clinical efficacy in treating CIS [33]. However, there is a lack of research on the relationship between the components of *A. coreanum* and efficacy in treating CIS. In this study, the UPLC-QE-MS analysis found that after administration of *A. coreanum*, 22 prototype components were detected in the plasma of gerbils. Among them, Guanfu base A

Table 2
Identification of compounds in *A. coreanum* and blood after administration of *A. coreanum*.

	Chamcterization	Formula	Calculated (*m/z*)	$[M+H]^+$ (*m/z*)	Error (ppm)	RT (min)	MS^2
1	Niacin [14]	$C_6H_5NO_2$	124.0393	124.0391	−1.61	0.24	124,80
2	Melibiose[a] [14]	$C_{12}H_{22}O_{11}$	365.1054	365.1047	−1.92	0.46	365,203,185
3	Guanfu base AA [15]	$C_{20}H_{27}NO_4$	346.2013	346.2003	−2.89	0.48	346,328,282
4	Delfissinol [16]	$C_{20}H_{27}NO_3$	330.2064	330.2056	−2.42	0.49	330,312,294
5	Hordenine [16]	$C_{10}H_{15}NO$	166.1226	166.1223	−1.81	0.56	166,122
6	Adenosine [15,17]	$C_{10}H_{13}N_5O_4$	268.1040	268.1035	−1.86	0.57	268,136
7	Senbusine A [18–20]	$C_{23}H_{37}NO_6$	424.2694	424.2690	−0.94	0.61	424,406,388,374,356,344
8	Guanfu base Q[a] [15]	$C_{22}H_{27}NO_5$	386.1962	386.1952	−2.59	0.62	386,368,308,280
9	Karakoline [17]	$C_{22}H_{35}NO_4$	378.2639	378.2629	−2.64	0.62	378,360,342,183,145
10	Genicunine [18–20]	$C_{22}H_{35}NO_4$	378.2639	378.2628	−2.91	0.63	378,360,342,183,145
11	Guanfu base U[a] [15]	$C_{20}H_{25}NO_4$	344.1856	344.1848	−2.32	0.63	344,326,308,298
12	Hetisine[a] [15,20,21]	$C_{20}H_{27}NO_3$	330.2064	330.2054	−3.03	0.65	330,312,294
13	Foresticine [19]	$C_{24}H_{39}NO_6$	438.2850	438.2840	−2.28	0.68	438,406,388,370, 356,338, 324,154,72
14	Guanfu base T[a] [15]	$C_{20}H_{25}NO_4$	344.1856	344.1848	−2.32	0.68	344,326,308
15	Anthoroisine F [22]	$C_{20}H_{27}NO_2$	314.2115	314.2101	−4.46	0.69	314,296,278
16	Tangutimine [16]	$C_{20}H_{27}NO_2$	314.2115	314.2101	−4.46	0.69	314,296,121
17	Songormine [18,20,23]	$C_{22}H_{29}NO_3$	356.2220	356.2210	−2.81	0.72	356,296
18	11-acetylhetisine [16]	$C_{22}H_{29}NO_4$	372.2169	372.2161	−2.15	0.75	372,312
19	Guanfu base I[a] [16]	$C_{22}H_{29}NO_5$	388.2118	388.2106	−3.09	0.78	388,328,310
20	Guanfu base W[a] [15]	$C_{22}H_{29}NO_5$	388.2118	388.2106	−3.09	0.78	388,328,310,282
21	Guanfu base K [15,24]	$C_{20}H_{27}NO_4$	346.2013	346.2006	−2.02	0.79	346,328,310,282
22	Hetisinone [16–18]	$C_{20}H_{25}NO_3$	328.1907	328.1900	−2.13	0.79	328,310,282
23	Guanfu base V [15–17]	$C_{20}H_{25}NO_3$	328.1907	328.1902	−1.52	0.80	328,310,292,282
24	Guanfu base A[a] [15,16]	$C_{24}H_{31}NO_6$	430.2224	430.2215	−2.09	0.81	430,370,310,292,264
25	Ignavined [19]	$C_{25}H_{39}NO_6$	450.2850	450.2841	−2.00	0.82	450,432,414,400,372,340,322
26	Isotalatizidine[a] [20,23,25]	$C_{23}H_{37}NO_5$	408.2744	408.2737	−1.71	0.84	408,390,376,372,362,358
27	Tanwusine [16]	$C_{20}H_{27}NO_3$	330.2064	330.2057	−2.12	0.86	330,312,294
28	N-ethylhokbusine B [17]	$C_{24}H_{37}NO_5$	420.2744	420.2743	−0.24	0.90	420,402,384,370,342,324
29	Acoridine[a] [15]	$C_{23}H_{31}NO_5$	402.2275	402.2270	−1.24	0.94	402,328,310,292,264
30	Condelphine[a] [15]	$C_{25}H_{39}NO_6$	450.2850	450.2842	−1.78	0.98	450,432,400,372
31	N-methyl-laurotetanine[a] [17,23]	$C_{20}H_{23}NO_4$	342.1700	342.1698	−0.58	0.98	342,311,297,265,279
32	Guanfu base O [15,24]	$C_{25}H_{33}NO_6$	444.2381	444.2368	−2.93	1.01	444,370,310,292,264
33	Sachaconitine [18]	$C_{23}H_{37}NO_4$	392.2795	392.2790	−1.27	1.01	392,360,342
34	Isocorydine [14]	$C_{20}H_{23}NO_4$	342.1700	342.1686	−4.09	1.06	342,219,58
35	Atisines [16]	$C_{22}H_{33}NO_2$	344.2584	344.2574	−2.90	1.15	344,326
36	Denudatine [18,20,23]	$C_{22}H_{33}NO_2$	344.2584	344.2574	−2.90	1.16	344,326,209
37	Guanfu base F nitrogen oxide compound [15]	$C_{26}H_{35}NO_7$	474.2486	474.2472	−2.95	1.22	474,368,326,308,280
38	Talatizamine[a] [18–20,23]	$C_{24}H_{39}NO_5$	422.2901	422.2888	−3.08	1.31	422,390,372,358
39	Guanfu base Z[a] [15,16]	$C_{24}H_{33}NO_5$	416.2431	416.2420	−2.64	1.32	416,328,310,292,264
40	Cumarin [14]	$C_9H_6O_2$	147.0441	147.0437	−2.72	1.37	147,119,91
41	Ferulic acid [15]	$C_{10}H_{10}O_4$	195.0652	195.0648	−2.05	1.39	195,177,149,145
42	Guanfu base X [15,17]	$C_{22}H_{29}NO_6$	404.2067	404.2055	−2.97	1.46	404,386,308
43	2-Isobutyryl-14-hyhroxy-hetisine-N-oxide [24]	$C_{24}H_{33}NO_6$	432.2381	432.2370	−2.54	1.75	432,326,308,280
44	Coreanine B [15]	$C_{25}H_{35}NO_5$	430.2588	430.2590	0.46	1.79	430,328,310,292,264
45	Benzoylmesaconine [18]	$C_{31}H_{43}NO_{10}$	590.2960	590.2949	−1.86	1.84	590,105
46	1-Dehydroneoline [19]	$C_{24}H_{37}NO_6$	436.2694	436.2665	−6.65	1.85	436,404,372
47	Guanfu base F [24]	$C_{26}H_{35}NO_6$	458.2537	458.2526	−2.40	1.90	458,380,292,264
48	Napelline [17,18]	$C_{22}H_{33}NO_3$	360.2533	360.2524	−2.50	2.03	360,342,324
49	14-Acetyltalatizamine[a] [19,20,23]	$C_{26}H_{41}NO_6$	464.3007	464.2997	−2.15	2.11	464,432,414,400,382,372,354,340
50	8-Deoxy-14-dehydro-aconosine [20]	$C_{22}H_{33}NO_3$	360.2533	360.2523	−2.78	2.24	360,342,324
51	Dictysine [20,23]	$C_{21}H_{33}NO_3$	348.2533	348.2511	−6.32	2.27	348,330,312
52	*Trans-p*-Hydroxycinnamic acid[a] [15]	$C_9H_8O_3$	165.0546	165.0543	−1.82	2.37	165,147,119
53	14-Benzoylhypaconine [17]	$C_{32}H_{45}NO_{10}$	604.3116	604.3105	−1.82	2.46	604,586,504
54	Coreanine C[a] [15]	$C_{26}H_{35}NO_6$	458.2537	458.2522	−3.27	2.52	458,370,310,292,264
55	Guanfu base G[a] [15]	$C_{26}H_{33}NO_7$	472.2330	472.2317	−2.75	2.54	472,412,352,292,264
56	Coreanine A[a] [15]	$C_{27}H_{37}NO_6$	472.2694	472.2698	0.85	2.70	472,370,310,292,264
57	Triacetylhetisine[a] [22]	$C_{26}H_{33}NO_6$	456.2381	456.2371	−2.19	3.02	456,396
58	Guanfu base R[a] [15]	$C_{27}H_{35}NO_7$	486.2486	486.2473	−2.67	3.16	486,426,394,352,292,264
59	Benzoylaconitine [23]	$C_{32}H_{45}NO_{10}$	604.3116	604.3104	−1.99	3.41	604,586
60	19-dihydroxyhetisan [19]	$C_{31}H_{35}NO_8$	550.2435	550.2418	−3.09	3.53	550,532,490,428,368,350,308
61	Guanfu base P[a] [13]	$C_{28}H_{37}NO_7$	500.2643	500.2627	−3.20	3.56	500,412,352,292,264
62	Songorine [23,25]	$C_{22}H_{31}NO_3$	358.2377	358.2370	−1.95	3.60	358,340,312,322
63	Karakanine [19]	$C_{22}H_{33}NO_4$	376.2482	376.2475	−1.86	3.66	376,358,340

(*continued on next page*)

Table 2 (*continued*)

	Chamcterization	Formula	Calculated (m/z)	$[M+H]^+$ (m/z)	Error (ppm)	RT (min)	MS^2
64	Coreanine D [15]	$C_{31}H_{35}NO_7$	534.2486	534.2474	−2.25	3.67	534,474,412,352,292,264
65	Trichodelphinine [22]	$C_{24}H_{31}NO_5$	414.2275	414.2265	−2.41	3.73	414,396
66	10-OH-mesaconitine [20]	$C_{33}H_{45}NO_{12}$	648.3015	648.2997	−2.78	3.97	648,588,338
67	Beiwutine [15,17,18]	$C_{33}H_{45}NO_{12}$	648.3015	648.2996	−2.93	4.17	648,588,338
68	Mesaconitine [20,25]	$C_{33}H_{45}NO_{11}$	632.3065	632.3060	−0.79	4.19	632,572,354
69	12-epi-napelline [20,23]	$C_{22}H_{33}NO_3$	360.2533	360.2525	−2.22	4.32	360,342,216
70	14-O-anisoylneoline [19]	$C_{32}H_{45}NO_8$	572.3218	572.3212	−1.05	4.53	572,484,456,424,400,382,340,322,294
71	Hypaconitine [15,25]	$C_{33}H_{45}NO_{10}$	616.3116	616.3109	−1.14	4.55	616,556,338,105
72	Neojiangyouaconitine [19,20]	$C_{33}H_{47}NO_9$	602.3324	602.3309	−2.49	4.93	602,416,370,338
73	Foresaconitine [18,23]	$C_{35}H_{49}NO_9$	628.3480	628.3456	−3.82	5.20	628,596,540
74	Hokbusine B [18]	$C_{22}H_{33}NO_5$	392.2431	392.2416	−3.82	5.51	392,374
75	8-O-cinnamoylneoline [17]	$C_{33}H_{45}NO_7$	568.3269	568.3261	−1.41	5.54	568,536
76	6-demethoxy-benzoylneoline [19]	$C_{30}H_{41}NO_7$	528.2956	528.2943	−2.46	5.76	528,510,324
77	16-β-hydroxycardiopetaline [25]	$C_{21}H_{33}NO_4$	364.2483	364.2472	−3.02	7.25	364,346,328,304
78	Linoleic acid [15,18]	$C_{18}H_{32}O_2$	281.2475	281.2454	−7.47	8.46	281,263,207
79	Delgrandine [18]	$C_{41}H_{43}NO_{12}$	742.2858	742.2845	−1.75	8.94	742,620
80	2-Methoxycinnamic acid [14]	$C_{10}H_{11}O_3$	161.0597	161.0594	−1.86	12.24	161,105,103,79

[a] Means that the component was detected in the plasma.

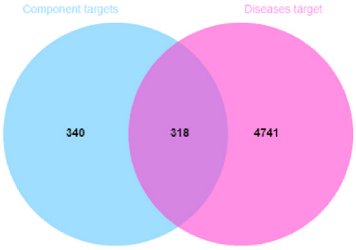

Fig. 5. Venn diagram of targets of prototype compounds absorbed in blood of *A. coreanum* and CIS.

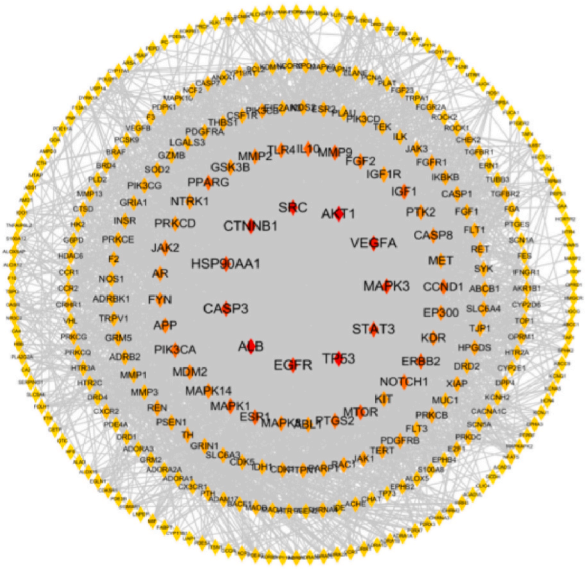

Fig. 6. PPI network of potential targets for *A. coreanum* treating CIS.

was an indicator component in A. coreanum, and research shown that it had anti-inflammatory and analgesic effects. It could enhance hypoxia resistance abilities [34]. These effects were related to those of anti-CIS drugs. Component-target-pathway network diagram analysis indicated that there was a strong correlation between these prototype components absorbed into blood and CIS related targets. The results of bioinformatics analysis indicated that *A. coreanum* had a "multi-component, multi-target" characteristic in treating CIS.

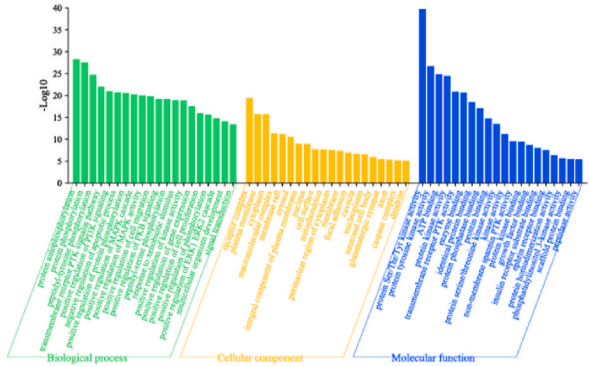

Fig. 7. GO function analysis of potential targets for *A. coreanum* treating CIS.

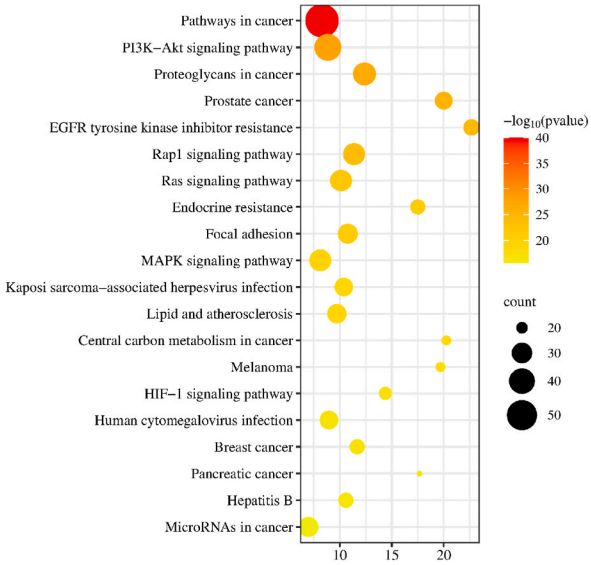

Fig. 8. KEGG signaling pathway enrichment analysis of potential targets for *A. coreanum* treating CIS.

Among numerous experimental animal species, gerbils have gradually become an emerging and mainstream model for screening brain protective active ingredients or drugs due to their unique brain structure [35–37]. From the perspective of brain physiological structure, due to congenital physiological defects, 90 % of Mongolian gerbils have a defect in the posterior communicating branch of the cerebral basal artery ring, without a posterior communicating artery connecting the internal carotid artery system and the basal artery system, which cannot form a complete cerebral basal artery ring (Willis ring) [38,39]. Based on this feature, using gerbils for unilateral carotid artery ligation to replicate an CIS model is simple and easy to operate. In recent years, it has been widely used in studying various pathological changes in the brain after cerebral ischemia and the neuroprotective effects of drugs [40,41]. In this study, neurological function and TTC results indicated that using unilateral ligated the carotid artery in gerbils can effectively replicate the CIS model. The gerbils after modeling had severe cerebral ischemia and exhibited significant neurological deficits such as facial paralysis, limb weakness, and abnormal movement. In this study, permanent ligation of the right carotid artery in gerbils was used as modeling method, prolonged ischemia time could also lead to gradual ischemia of the contralateral brain [42,43]. This discovery suggested that for sudden CIS, timely treatment should be taken to avoid worsening of cerebral ischemia. However, further exploration was needed to evaluate the state of ischemia on the non-infarcted and infarcted side.

The acute inflammatory response caused by CIS plays an important role in cerebral ischemic injury [44]. The current research demonstrated that the main mechanism involved in post ischemic inflammatory response was the production of TNF-α by ischemic neurons, and the large number of regulatory factors produced by inflammatory cells and damaged neurons. The activation of the intracellular second messenger system, the increase of oxygen free radicals and hypoxia itself triggered the gene expression of a large number of preinflammatory mediators by inducing the synthesis of transcription factors. In this way, damaged brain cells produced a large amount of inflammatory mediators such as platelet activating factor (PAF), TNF-α, IL-1β and IL-6, which caused white blood cells to infiltrate local ischemic brain tissue [45,46]. CIS caused inflammatory, which could be detected both in the brain and serum of gerbils, promoting the production of inflammatory factors. After treatment with *A. coreanum*, the levels of inflammatory factors

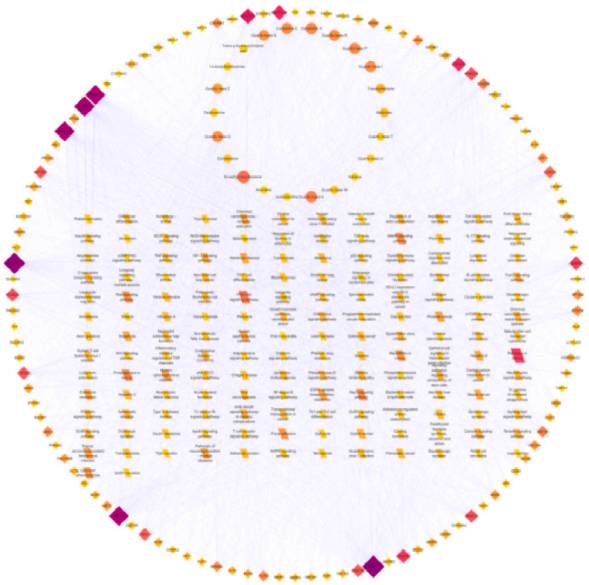

Fig. 9. Component-target-pathway network diagram A. coreanum treated gerbils with CIS by regulating PI3k/Akt pathway.

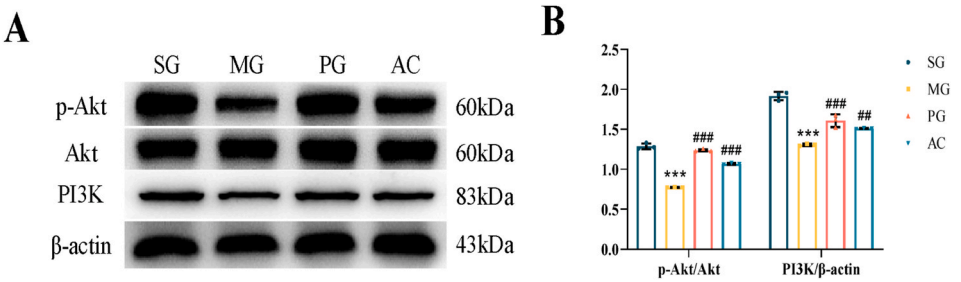

Fig. 10. Western blotting analyses of PI3K and *p*-Akt. A: The protein levels of brian PI3K and *p*-Akt B: Quantified levels of PI3K and *p*-Akt (Compared with SG, $^{***}P < 0.001$; Compared to MG, $^{\#\ \#}P < 0.01$,$^{\#\ \#\ \#}P < 0.001$).

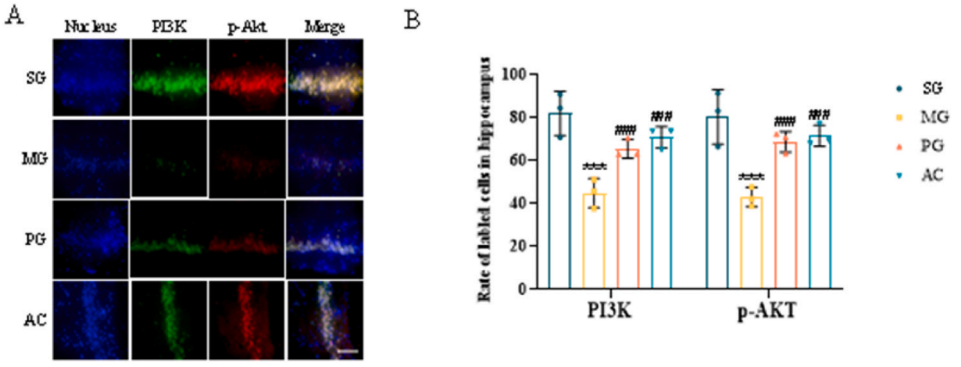

Fig. 11. Immunofluorescence analyses of PI3K and *p*-Akt in the CA1 region of gerbil hippocampus. A: The protein levels of neurocyte PI3K and *p*-Akt (Scale bar: 20 μm) B: Quantified levels of PI3K and *p*-Akt
(Compared with SG, $^{***}P < 0.001$; Compared to MG, $^{\#\ \#}P < 0.001$).

decreases, indicating that *A. coreanum* inhibited the inflammatory response caused by CIS. Meanwhile, compared to MG, the levels of TNF-α and IL-6 in brain of AC reduced compared to those in serum, indicating that *A. coreanum* exert anti-inflammatory effects in the brain, the focus of CIS.

The PI3K/Akt signaling pathway was an intracellular signaling pathway that responded to extracellular signals and promoted

metabolism, proliferation, cell survival, growth, and angiogenesis [47,48]. In the KEGG database, there were up to 71 types of pathways directly related to the PI3K/Akt signaling pathway, which were involved in the occurrence and development of CIS as one of the key cascade signaling pathways. It played a core role in various mechanisms such as cell apoptosis, autophagy, oxidative stress, and inflammatory response [49,50]. After activation PI3K promoted the phosphorylation of AKT, making it activated. Therefore, the activity of PI3K was usually reflected through the level of phosphorylation of AKT. The phosphorylated Akt (*p*-Akt) regulated the downstream of the signaling pathway. The bioinformatics analysis results in this study also indicated that the main pathway for treating CIS with *A. coreanum* included PI3K/Akt signaling pathway. According to the results of western blotting and immunofluorescence, *A. coreanum* activated the expression of PI3K and *p*-Akt on the PI3K/Akt signaling pathway. And the results of immunofluorescence also shown that *A. coreanum* not only increased the expression of related proteins, but also had a good repair effect on damaged hippocampal CA1 neurons, indicating that the mechanism of *A. coreanum* in treating CIS was multiple.

The research results at this stage also cause us some new thoughts. *A. coreanum* also affected related proteins on the KEAP1-Nrf2 signaling pathway to treat CIS based on the results of our group, but this signaling pathway was not predicted in the bioinformatics analysis results. This might be due to the lack of research on the relationship between *A. coreanum* or CIS and this pathway, which was the disadvantage of bioinformatics analysis at the moment. We will conduct in-depth research on this in the future. In addition, in the PI3K/Akt signaling pathway, PI3K can catalyze the generation of PIP2 to PIP3 after activation, thereby promoting partial activation of Akt. This study has confirmed the regulatory effect of *A. coreanum* on *p*-Akt, but it needs further study on the effect of p-PI3K, and it needs to be verified by adding inhibitor groups.

This study preliminarily confirmed that *A. coreanum* treated CIS through the PI3K/Akt signaling pathway. Based on the results of bioinformatics and immunofluorescence results, the mechanism of *A. coreanum* in treating CIS was not only related to inhibiting inflammatory reactions, but also to oxidative stress, repairing nerve cells, and other aspects. Thus further research is needed to verify the "multi-component, multi-target" mechanism of *A. coreanum* in treating stroke.

6. Conclusion

A. coreanum inhibited inflammatory response by activating PI3K/Akt signaling pathway, reduced the area of cerebral infarction, and enhancing the activity of neuronal cells in the CA1 area of the hippocampus on gerbils with CIS. *A. coreanum* had a therapeutic effect on CIS. And the diterpenoid alkaloids were related to this effect.

Research funding

This research was supported from the fundings of the China National Natural Science Foundation (81973478), the Liaoning Revitalization Talents Programme (XLYC2002004), and Basic Scientific Research Project of Universities of Liaoning Provincial Education Department (2023).

Animal ethics review

All animal studies were approved by the Animal Ethics Committee at the Affiliated Hospital of Liaoning University of Traditional Chinese Medicine (Approval No. 2019 YS (DW) -028-0).

Data availability statement

The data associated with the study not been deposited yet into a publicly available repository. If you have any needs, please contact the corresponding author by email to obtain more information about the data.

CRediT authorship contribution statement

Ru Jia: Writing - original draft, Visualization, Validation, Software, Methodology, Investigation, Data curation, Conceptualization. **Qian Cai:** Writing - review & editing, Validation, Supervision, Investigation, Funding acquisition, Formal analysis, Conceptualization. **Yang Qu:** Writing - review & editing, Supervision, Methodology, Data curation, Conceptualization.

Declaration of competing interest

The authors declare that they have no known competing financial interests or personal relationships that could have appeared to influence the work reported in this paper.

Appendix A. Supplementary data

Supplementary data to this article can be found online at https://doi.org/10.1016/j.heliyon.2024.e24008.

References

[1] Global, regional, and national burden of stroke and its risk factors, 1990-2019: a systematic analysis for the Global Burden of Disease Study 2019 [J]. The Lancet, Neurology 20 (10) (2021) 795–820, https://doi.org/10.1016/S1474-4422(21)00252-0.

[2] W. Wang, et al., Prevalence, incidence, and mortality of stroke in China: results from a nationwide population-based survey of 480687 adults [J], Circulation 135 (8) (2017) 759–771, https://doi.org/10.1161/CIRCULATIONAHA.116.025250.

[3] A. Algra, et al., Stroke in 2016: stroke is treatable, but prevention is the key [J], Nat. Rev. Neurol. 13 (2) (2017) 78–79, https://doi.org/10.1038/nrneurol.2017.4.

[4] R. Shi, et al., Experimental study of effect of yiqi huoxue huazhou jiedu formula on cerebral ischemia-reperfusion injury in rats based on Nrf2/HO-1 pathway [J], J. Hebei Traditional Chin. Med. Pharmacol. 38 (1) (2023) 3–8+23, https://doi.org/10.16370/j.cnki.13-1214/r.2023.01.013.

[5] X.X. Li, et al., Protective effect and mechanism of extract from Tribulus terrestris fruit on ischemic stroke rats based on UPLC-Q-Exactive-MS metabolomics technology[J/OL], Special Wild Econ. Anim. Plant Res. (7) (2023) 1–7, https://doi.org/10.16720/j.cnki.tcyj.2023.016.

[6] Q. Chen, et al., Effect of paeonol on improving behavioral dysfunction in a mouse model of middle cerebral artery occlusion [J], Chin. General Pract. 26 (27) (2023) 3441–3449.

[7] Y. Wang, et al., UPLC-Q-TOF-MS/MS technology combined with network pharmacology to explore the mechanism of the treatment of ischemic stroke with Zhongfeng Yure Formula [J], J. Chin. Med. Mater. 45 (12) (2022) 2904–2910, https://doi.org/10.13863/j.issn1001-4454.2022.12.021.

[8] M. Zhu, et al., Protection mechanism of zhongfeng huichun tablets on ischemic stroke [J], J. Chin. Prescr. Drug 20 (12) (2022) 38–40.

[9] Chinese Pharmacopoeia Committee, in: Pharmacopoeia of the People's Republic of China [S], China Medical Science Press, Beijing, China, 1977, p. 243, 1977.

[10] H.J. Tao, et al., List of Famous Doctors [M], vol. 6, People's Health Publishing House, 1986, p. 232.

[11] Editorial board of Chinese materia medica of national administration of traditional Chinese medicine. Chinese materia medicaa: 3rd secti [M], Shanghai Scientific and Technical Publishers (1999) 123–128.

[12] Y.Y. Huang, Yuqiu medicine solution [M], The Medicine Science and Technology Press of China 1 (2017) 9.

[13] Yang Tan, Yang's Family Collection Prescription [M], People's Health Publishing House, 1988, p. 18, 06.

[14] L. Zhang, et al., Study on cartilage protective effect of xibining on KOA model rats based on UPLC-Q-orbitrap MS/MS technique [J], Journal of Nanjing University of Traditional Chinese Medicine 39 (1) (2023) 32–41, https://doi.org/10.14148/j.issn.1672-0482.2023.0032.

[15] X.Y. Xu, et al., Comparative Study of Chemical Composition and Pharmacodynamics before and after Processing [D], Liaoning University of Traditional Chinese Medicine, 2021.

[16] Y. Wang, et al., Anti-acetylcholinesterase active ingredients from Aconitum tanguticum by UPLC-Q-TOF-MS/MS [J], Chin. J. Exp. Tradit. Med. Formulae 27 (20) (2021) 130–137, https://doi.org/10.13422/j.cnki.syfjx.20211446.

[17] W. Xu, Application of Liquid Mass Spectrometry in the Analysis of Two Traditional Chinese Medicine Components [D], Guangzhou University of Traditional Chinese Medicine, 2015.

[18] X.T. Ye, et al., Analysis of chemical constituents of Aconiti Radix and its different processed products based on UPLC/Q-TOF-MS/MS [J], China Journal of Traditional Chinese Medicine and Pharmacy 36 (10) (2021) 5837–5842.

[19] Q. Fan, et al., Diterpenoid alkaloids of the processed products of aconiti lateralis radix praeparata based on UPLC-Q-TOF-MS/MS and GNPS [J], Acta Sci. Nat. Univ. Sunyatseni 60 (3) (2021) 30–44, https://doi.org/10.13471/j.cnki.acta.snus.2020.01.20.2020c004.

[20] Y.X. Qin, et al., Components in radix aconiti before and after processing by using HPLC-MS [J], Journal of Beijing University of Traditional Chinese Medicine 39 (4) (2016) 298–303.

[21] Y. Chen, et al., Components analysis of shangshi qutong plaster by UPLC-orbitrap-MSn and study on its anti-oxidant and anti-inflammatory effects [J], Information on Traditional Chinese Medicine 38 (8) (2021) 14–22, https://doi.org/10.19656/j.cnki.1002-2406.210802.

[22] J.P. Xu, Studies on Diterpenoid Alkaloids from Delphinium Grandiflorum, Aconitum Bulbilliferum, Aconitum Hemsleyanum Var. Circinatum and Aconitum Coreanum [D], Southwest Jiaotong University, 2021, https://doi.org/10.27414/d.cnki.gxnju.2021.003248.

[23] L. Wang, et al., Comparative study on unprocessed aconiti radix and unprocessed aconiti lateralis radix by UPLC-MS^n [J], Chinese Journal of Pharmaceutical Analysis 37 (9) (2017) 1640–1647, https://doi.org/10.16155/j.0254-1793.2017.09.14.

[24] B.N. Xing, et al., Identification of diterpenoid alkaloids in the roots of cultured Aconitum coreanum by HPLC-Q-TOF-MS [J], J. China Pharm. Univ. 45 (2) (2014) 192–199.

[25] H. Li, et al., Rapid screening of bufadienolides and diterpenoid alkaloids in huoxin pills by molecular weight imprinting [J], Modern Chinese Medicine 24 (12) (2022) 2350–2363, https://doi.org/10.13313/j.issn.1673-4890.20220702001.

[26] Z.L.Y.T. Yusupu, et al., Study on the pathogenesis of acute ischemic stroke [J], Cardiovascular Disease Electronic Journal of Integrated Traditional Chinese and Western Medicine 1 (2020) 15+40, https://doi.org/10.16282/j.cnki.cn11-9336/r.2020.01.009.

[27] Y.H. Song, The value of aspirin combined with clopidogrel in theTreatment of acute ischemic stroke [J], Journal of Mathematical Medicine 35 (9) (2022) 1384–1386.

[28] J.M. Huo, et al., Clinical efficacy and safety analysis of different thrombolytic treatments for acute ischemic stroke patients [J], J. Prev. Med. Chin. People's Liberation Army 34 (S2) (2016) 271–272, https://doi.org/10.13704/j.cnki.jyyx.2016.s2.244.

[29] H.B. Hao, Effect of thrombolytic therapy with low-dose Urokinase in patients with acute ischemic stroke [J], Guide of China Medicine 10 (34) (2012) 236–237, https://doi.org/10.15912/j.cnki.gocm.2012.34.452.

[30] Xing, et al., New diterpenoid alkaloids from Aconitum coreanum and their anti-arrhythmic effects on cardiac sodium current.[J], Fitoterapia 94 (2014), https://doi.org/10.1016/j.fitote.2014.01.022.

[31] Y.J. Li, et al., Effects of Guanfu total base on Bcl-2 and Bax expression and correlation with atrial fibrillation[J], Hellenic J. Cardiol. 59 (5) (2018), https://doi.org/10.1016/j.hjc.2018.02.009.

[32] Huang, et al., Comparative effects of Guanfu base A and Guanfu base G on HERG K+ channel.[J], J. Cardiovasc. Pharmacol. 59 (1) (2012), https://doi.org/10.1097/FJC.0b013e318236e380.

[33] Y. TianPeng, et al., Aconitum coreanum Rapaics: botany, traditional uses, phytochemistry, pharmacology, and toxicology [J], Open Chem. 20 (1) (2022) 1263–1282, https://doi.org/10.1515/CHEM-2022-0235.

[34] Y. Jiang, et al., Pharmacological studies on Guanfu base A[J], Chin. Tradit. Herb. Drugs 18 (10) (1987) 23–26.

[35] C. Park, et al., Effects of long-term exercise on memory recovery in the aged gerbil hippocampus after transient cerebral ischemia, Crit. Care 19 (S1) (2015) 464, https://doi.org/10.1186/cc14544.

[36] L. Anita, et al., Validation of the reference genes for expression analysis in the Hippocampus after transient ischemia/reperfusion injury in gerbil brain [J], Int. J. Mol. Sci. 24 (3) (2023), https://doi.org/10.3390/IJMS24032756, 2756-2756.

[37] L. TaeKyeong, et al., Ischemia-Reperfusion under hyperthermia increases heme oxygenase-1 in pyramidal neurons and astrocytes with accelerating neuronal loss in gerbil Hippocampus [J], Int. J. Mol. Sci. 22 (8) (2021), https://doi.org/10.3390/IJMS22083963, 3963-3963.

[38] S.M. Liu, et al., Advances in application of gerbil models of cereoral ischemia and their advantages and disadvantages [J], Acta Lab. Anim. Sci. Sin. 21 (6) (2013) 79–83.

[39] J.H. Li, et al., The progress in morphological study in global ischemia of gerbils [J], Prog. Anat. Sci. (4) (2006) 366–370, https://doi.org/10.16695/j.cnki.1006-2947.2006.04.023.

[40] Y.L. Gao, et al., Influence of Qingnaopian tablet on plasma ET and CGRP content and brain tissue pathological changes in gerbil cerebral ischemia reperfusion model[J], Practical Journal of Medicine & Pharmacy 35 (1) (2018) 47–50, https://doi.org/10.14172/j.issn1671-4008.2018.01.018.

[41] Q.J. Shi, et al., Cysteinyl leukotriene receptor antagonist alleviates global cerebral ischemia/reperfusion injury in gerbils through down-regulating autophagy [J], Acta Lab. Anim. Sci. Sin. 26 (1) (2018) 57–64.

[42] S. Cheng, et al., Gelsemine exerts neuroprotective efects on neonatal mice with hypoxic-ischemic brain injury by suppressing infammation and oxidative stress via Nrf2/HO-1 pathway[J], Neurochem. Res. 48 (2023) 1305–1319.
[43] W. Zeng, et al., Bone marrow mesenchymal stem cells overexpressing hepatocyte growth factor ameliorate hypoxic-ischemic brain damage in neonatal rats[J], Transl. Neurosci. 12 (2021) 561–572.
[44] ZhengZ. YenariMA, Post-ischemic inflammation: mole-cular mechanisms and therapeutic implicationslJl Neurol [J], Rcs 26 (8) (2004) 884–892.
[45] Y.T. An, et al., The pathogenesis of cerebral ischemia and its treatment [J], World Clinical Drug 31 (1) (2010) 35–39.
[46] Y.H. Liu, W. Fang, Research progress on the pathogenesis of ischemic stroke [J], China Modern Doctor 48 (25) (2010) 11–12.
[47] H. Chen, et al., PI3K/AKT research progress on PI3K/AKT signaling pathway in programmed cell death after ischemic stroke [J,]. Pharmacology and Clinics of Chinese Materia Medica 38 (2) (2022) 247–252, https://doi.org/10.13412/j.cnki.zyyl.20210806.002.
[48] H. Bai, et al., Research progress on the mechanism of acupuncture regulating PI3K/Akt signaling pathway to intervene in centralnervous systemdiseases [J], Global Traditional Chinese Medicine 14 (8) (2021) 1546–1550.
[49] S. ChangSheng, et al., MicroRNA-204-5p ameliorates neurological injury via the EphA4/PI3K/AKT signaling pathway in ischemic stroke [J], ACS Chem. Neurosci. (2023), https://doi.org/10.1021/ACSCHEMNEURO.3C00047.
[50] W. Yuanyuan, et al., Inhibition of PI3K/Akt/mTOR signaling by NDRG2 contributes to neuronal apoptosis and autophagy in ischemic stroke [J], J. Stroke Cerebrovasc. Dis. 32 (3) (2023), https://doi.org/10.1016/J.JSTROKECEREBROVASDIS.2023.106984, 106984-106984.